Image magnified lensless holographic projection by convergent spherical beam illumination

Chenliang Chang (常琛亮)[1,2,*], Yijun Qi (祁怡君)[2], Jun Wu (吴 俊)[2], Jun Xia (夏 军)[2], and Shouping Nie (聂守平)[1]

[1]*Jiangsu Key Laboratory for Opto-Electronic Technology, School of Physics and Technology, Nanjing Normal University, Nanjing 210023, China*

[2]*Joint International Research Laboratory of Information Display and Visualization, School of Electronic Science and Engineering, Southeast University, Nanjing 210096, China*

**Corresponding author: changchenliang@hotmail.com*

Received July 11, 2018; accepted August 27, 2018; posted online September 21, 2018

In liquid crystal spatial light modulator (SLM)-based holographic projection, the image is usually displayed at a distant projection screen through free space diffraction from a computer-generated hologram (CGH). Therefore, it allows for removing of the projection lens for the sake of system simplification and being aberration free, known as the "lensless holographic projection". However, the maximum size of the optical projected image is limited by the diffraction angle of the SLM. In this Letter, we present a method for the implementation of image magnification in a lensless holographic projection system by using convergent spherical wave illumination to the SLM. The complete complex amplitude of the image wavefront is reconstructed in a lensless optical filtering system from a phase-only CGH that is encoded by the off-axis double-phase method. The dimensions of the magnified image can break the limitation by the maximum diffraction angle of the SLM at a given projection distance. Optical experiment results with successful image magnification in the lensless holographic projection system are presented.

OCIS codes: 090.2870, 090.1760.
doi: 10.3788/COL201816.100901.

Attention to holographic projection has increased in the past decade. In a traditional holographic projector, the size of the projected images can be easily magnified through the imaging system, which involves zoom lenses. For example, the optical projected image could be magnified by using either the 4f system[1] or one lens with a divergent spherical illumination[2,3]. However, the existing projection lenses would increase the complexity of the projection system and introduce lens aberration.

Since in holographic projection the projected image is reconstructed via diffraction from the computer-generated hologram (CGH), the reconstructed distance and size of the image can be controlled digitally in the numerical calculation of Fresnel diffraction from the image to the CGH. Therefore, it allows abandoning bulks of imaging and zoom lenses, also referred as lensless holographic projection[4,5], and shows great potential in a variety of applications towards portable and miniature projection systems.

Generally, while the holographic projection is optically achieved by loading the CGH into a dynamic spatial light modulator (SLM), the concept of "lensless" in a holographic projection system could be classified into two categories according to the previously reported works. (1) There are absolutely no lenses in the whole optical setup[4–6], as shown in Fig. 1(a). In this type, the direct point light source with high divergence, such as an optical fiber, is usually used as the illumination source, allowing the realization of miniaturized holographic pico-projectors. (2) There are no lenses existing between the SLM and the projection screen, but a lens (or lenses) responsible for beam collimation could be permitted before illumination to the SLM[7–9], such as in the case shown in Fig. 1(b). Although the beam collimation lens is used, it can still be called a "lensless" holographic projection since the expression of "lensless" mainly refers to the substantive holographic projection process that happens between the SLM (CGH) and the screen via Fresnel diffraction. In this Letter, our work of lensless holographic projection is mainly focused on the second case.

In lensless holographic projection, the CGH that needs to be loaded into the SLM is calculated from the projected image at a given distance by using the Fresnel diffraction algorithms. The fast Fourier transforms (FFTs) used in the Fresnel diffraction calculation map the CGH in the SLM plane onto a target image in the image plane, and then, the image size is restricted by the diffraction angle of the used SLM. Due to the fact that the maximum diffraction angle depends on the pixel pitch of the SLM, the maximum reachable dimension of the projected image is determined by the so-called Nyquist criterion of

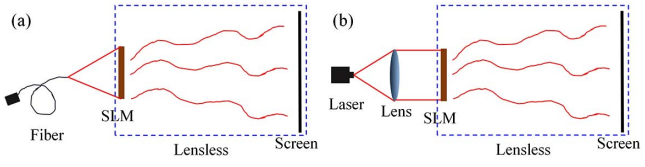

Fig. 1. Two cases for lensless holographic projection.

$L = \lambda z/\mathrm{d}x$, where λ is the light wavelength, z is the projection distance, and $\mathrm{d}x$ is the pixel pitch of the SLM. Shimobaba *et al.* proposed a method of lensless zoomable holographic projection, where the image size can be adjustable during the calculation of CGH by employing a convolution-based aliasing-reduced shifted and scaled (ARSS)-Fresnel diffraction algorithm[6,10]. Thus, the image can be magnified by presetting the image pixel pitch through diffraction calculation. An alternative method for adjusting image dimension in CGH calculation is also reported in Ref. [11] by using the double-step Fresnel diffraction algorithm. However, the maximum size of the image in both of these methods is still limited by the Nyquist criterion due to the restrictive diffraction angle of the SLM.

Using a spherical wave to illuminate the SLM is an effective solution to break the Nyquist criterion and enlarge the size of the reconstructed image. By introducing a spherical illumination wavefront, the diffraction angle of the SLM is increased, and the diffraction region occupied by the projected image is further enlarged. Qu *et al.* proposed a method for image magnification in lensless holographic projection[9]. The SLM is illuminated by a divergent spherical beam, and the size of the optical projected image can exceed the traditional Nyquist limit. But, the phase-only CGH used in the experiment is generated by the Gerschberg–Saxton (GS) algorithm[12], and the image would be degraded by the presence of speckle noise.

In this Letter, we propose an image magnified lensless holographic projection system. Instead of using a divergent beam, we use a convergent spherical wave illumination to increase the diffraction angle of the SLM, therefore enabling the dimension magnification of the projection image, as well as maintaining the high image quality of speckle noise suppression due to the reconstruction of complex amplitude of the image via a lensless optical filtering system. In this way, a large-sized and high-definition lensless holographic projection is achieved.

We first briefly review the principle of CGH calculation and reconstruction in previously reported lensless holographic projection systems[13], as illustrated in Fig. 2. For simplicity, the method is discussed in terms of a one-dimensional model. As shown in Fig. 2(a), the CGH is calculated based on the double-step Fresnel diffraction algorithm, in which a virtual immediate plane is established between the image and the CGH plane, assuming that the pixel pitch of the image and the CGH is $\mathrm{d}x$ and $\mathrm{d}h$, respectively. Prior to the diffraction calculation, the image is compulsively multiplied by a spherical convergent phase factor. This operation is equivalent to illuminating the image by a virtual convergent light in order to ensure the focus of the image wavefront into a spot at the virtual plane through diffraction. Thus, the added spherical phase factor can be written as

$$\varphi(x) = -\pi x^2/\lambda(z-d), \tag{1}$$

where λ is the wavelength. z and d are the distance from the CGH to the image and virtual plane, respectively.

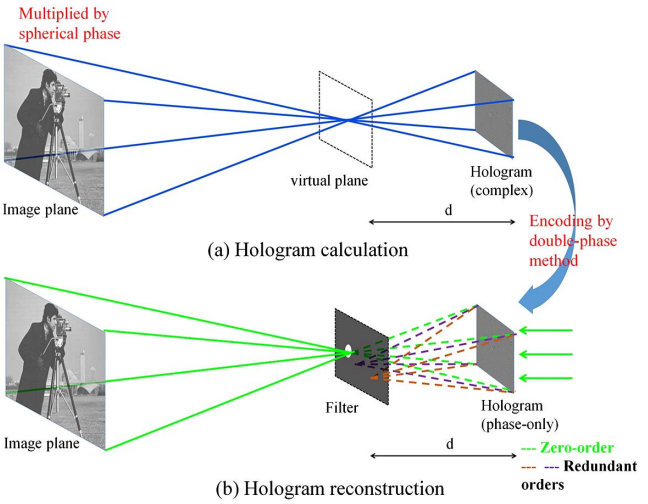

Fig. 2. Illustration of CGH calculation and reconstruction in lensless holographic projection system.

Then, the CGH can be calculated using two steps of Fresnel diffraction from the image[13]. First, the wavefront on the virtual plane is calculated by Fresnel diffraction of

$$V(x_\nu) = \int I(x) \cdot \exp\left[\frac{i\pi(x_\nu - x)^2}{\lambda(z-d)}\right]\mathrm{d}x. \tag{2}$$

Second, the wavefront of the CGH plane is obtained by continuously performing the Fresnel diffraction of

$$H(x_h) = \int V(x_\nu) \cdot \exp\left[\frac{i\pi(x_h - x_\nu)^2}{\lambda d}\right]\mathrm{d}x_\nu. \tag{3}$$

In Eqs. (2) and (3), $I(x)$, $V(x_\nu)$, and $H(x_h)$ denote the wavefront of the image, virtual plane, and CGH, respectively. The numerical calculation of Fresnel diffraction in Eqs. (2) and (3) can be accelerated by the existing FFT-based algorithms, i.e., the "ARSS-Fresnel diffraction" algorithm[10]. After the CGH is generated based on the double-step Fresnel diffraction calculation, we encode this complex CGH into a phase-only CGH using the off-axis double-phase method[14,15].

The reconstruction of the encoded phase-only CGH is an inverse process to the calculation. Since the phase-only CGH acts as a phase grating that encodes the complex amplitude $H(x_h)$ into its zero diffraction order, the complex amplitude of the image wavefront could be totally reconstructed by only selecting the zero-order diffraction component from the CGH using an aperture filter at the virtual plane due to the fact that the wavefront of zero-order diffraction would be focused into a spot at the virtual plane.

The principle of the proposed image magnification method in lensless holographic projection is described below. The reconstruction of the complex amplitude of the image is commonly realized by loading the phase-only CGH into the pixelated SLM. The SLM acts as a

diffractive optical element, and the diffraction angle of the modulated light beam obeys the formula of

$$\sin\theta_{\text{diff}} - \sin\theta_{\text{in}} \approx \theta_{\text{diff}} - \theta_{\text{in}} = \frac{\lambda}{2\text{d}h},$$
$$\theta_{\text{diff}} = \theta_{\text{in}} + \frac{\lambda}{2\text{d}h}, \tag{4}$$

where θ_{in} represents the angle of the incident illumination beam, and θ_{diff} represents the maximum diffraction angle after being modulated by the SLM. Conventionally, the incident angle is $\theta_{\text{in}} = 0$ since the SLM is illuminated by the collimated plane waves; so, the viewing angle $\theta = 2\theta_{\text{diff}} = \lambda/\text{d}h$ is mainly dependent on the pixel pitch $\text{d}h$ of the SLM, as shown in Fig. 3(a). The maximum reachable size of the projection image at a given distance (z) will be restricted by the typical commercial SLM, i.e., $\text{d}h = 8$ μm for the Holoeye Pluto-type phase-only SLM. Generally, the maximum size of the image can be calculated according to the Nyquist criterion as $L = \lambda z/\text{d}h$.

An obvious solution for the problem of breaking the limitation of the image size is to introduce an incident angle ($\theta_{\text{in}} \neq 0$) of the illumination beam while still maintaining the principle of complex amplitude modulation for high image quality as described above. This means that two necessary requirements should be satisfied at the same time: firstly, the plane wave illumination should be replaced by spherical wavefront illumination for the sake of increasing the diffraction angle; secondly, the beam after being modulated by the SLM should be focused into a spot at the virtual plane for further facilitated filtering operation. Based on these two requirements, the incident beam of the convergent spherical wavefront is an optimum adoption as the illumination. As illustrated in Fig. 3(b), by using convergent spherical wave illumination, the angle of the incident beam as well as the diffraction beam is both increased, thereby expanding the viewing angle (diffraction angle) according to the relation as $\theta = 2\theta_{\text{diff}} = 2\theta_{\text{in}} + \lambda/\text{d}h$. The phase of the spherical illumination on the SLM plane is determined by $\varphi(x_h) = -\pi x_h^2/\lambda f$ so as to be focused on the virtual plane. All of the incident light, especially in the corner part, from the SLM is guaranteed to converge to the spot without light loss under the illumination of the convergent spherical wave. So, the complete information for the complex image could be completely reconstructed with a larger size of $\lambda z/\text{d}h + 2z\theta_{\text{in}}$. In this way, the image can be magnified through breaking the Nyquist limitation of the SLM, owing to the introduction of the convergent spherical illumination under an incident angle of θ_{in}. It should be noted that owing to the producing of an extra spherical phase on the SLM, a correction should be performed by adding the CGH with the conjugated phase of the spherical illumination.

The image magnification in lensless holographic projection under spherical illumination is demonstrated in optical experiments. Figure 4 shows the sketch of the experimental setup. The laser illumination source (532 nm) is delivered by a convergent lens with a short focal lens, which shapes the beam into a convergent spherical wavefront to illuminate the phase-only SLM (Holoeye PLUTO, resolution 1920 × 1080 with pixel pitch of 8 μm). After being modulated by the encoded phase-only CGH, the beam then passes a low-pass filter consisting of a circular iris whose diameter is 3.3 mm. The complex amplitude of the image is reconstructed on a large projection screen with a smooth, flat surface to avoid extra diffusive speckles.

In order to compare the effect of image magnification by the proposed method, we first reconstruct the image by using plane wave illumination. Figure 5(a) shows the projection screen of a white board that is placed at distance $z = 2$ m from the SLM. The resolution of the test image "Monalisa" is 1920 × 1080. Figure 5(b) shows the result of the reconstructed image with size of 13.44 cm × 7.56 cm,

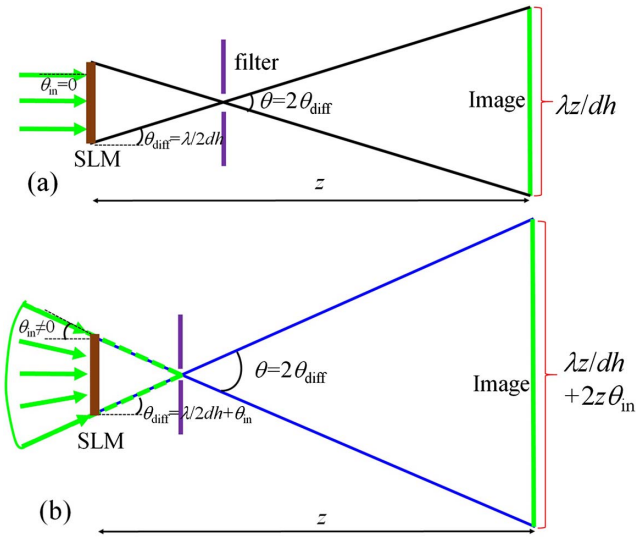

Fig. 3. Principle of image magnification by using spherical wave illumination. (a) Plane wave illumination, the maximum reachable image size is limited by Nyquist criterion. (b) Convergent spherical wave illumination, the image is reconstructed with a larger size due to the enlargement of the diffraction angle.

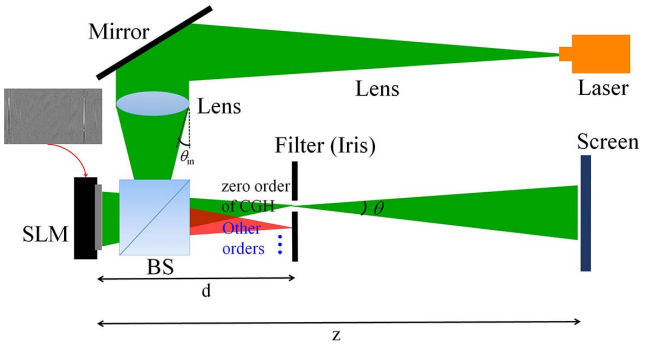

Fig. 4. Optical setup for lensless holographic projection using convergent spherical beam illumination.

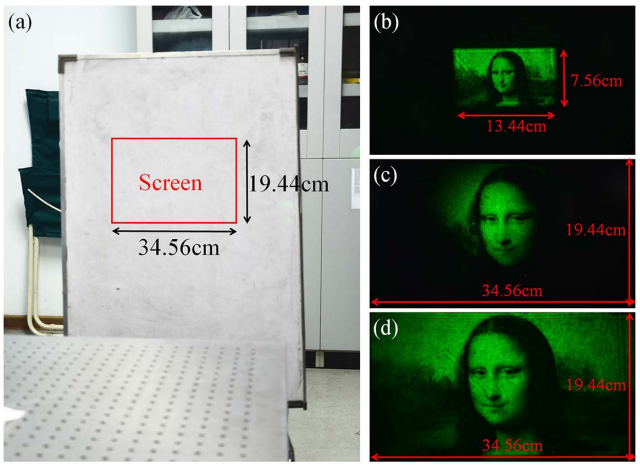

Fig. 5. (a) Projected screen marked with the size of the target projected image. (b) Reconstructed image under conventional plane wave illumination. (c) Reconstructed image with magnified size under conventional plane wave illumination. (d) Reconstructed image with magnified size under spherical wave illumination.

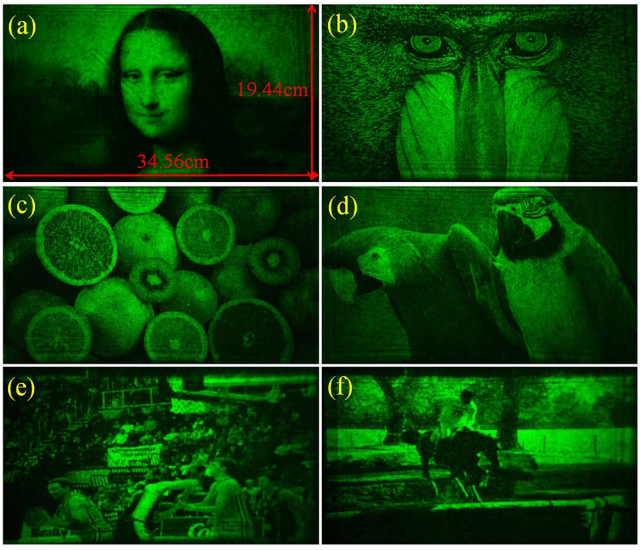

Fig. 6. Optical reconstructions of image magnified lensless holographic projection. (a)–(d) Monochromatic reconstructions of "Monalisa", "Baboon", "Fruits", and "Parrots" with image width of 34.56 cm and image height of 19.44 cm, respectively. (e) and (f) are one frame extracted from two 1080P high definition animations (Visualizations 1 and 2), respectively.

whose width (13.44 cm) is almost the maximum diffraction bandwidth limited by the diffraction angle of the SLM ($\lambda z/\mathrm{d}h$). In the CGH calculation of Fig. 5(b), the pixel pitch of the image is $\mathrm{d}x = 13.44\ \mathrm{cm}/1920 = 70\ \mu\mathrm{m}$. Next, we enlarge the pixel pitch of the image to $\mathrm{d}x = 180\ \mu\mathrm{m}$ in CGH calculation, thereby magnifying the size of the target image to 34.56 cm × 19.44 cm. The corresponding reconstruction from the SLM under plane wave illumination is shown in Fig. 5(c). The maximum diffraction angle of the SLM is limited by plane wave illumination, resulting in image content loss on the projection screen. The maximum size of the visible image content is restricted by the Nyquist criterion and the rest image contents are blocked by the filter. This problem is overcome by replacing the plane wave illumination with convergent spherical wave illumination using the setup displayed in Fig. 4. The lens position is adjusted to make sure that the incident beam focuses toward the SLM with an incident angle of $\theta_{\mathrm{in}} \approx 3°$. As expected, the reconstructed image shown in Fig. 5(d) is visible in the whole predesigned projection region [marked as red line in Fig. 5(a)] due to the enlargement of the diffraction angle of the SLM. The image size has been magnified approximately by 2.6 times (180 μm/70 μm) compared with the result of Fig. 5(b), which is reconstructed under conventional plane wave illumination, proving the image magnification in the holographic projection based on the proposed method. It is also noted that, although coherent illumination is used, the reconstructed image shows no significant speckle noise, owing to the fact that the smooth phase (spherical phase) distribution of the complex amplitude image is obtained, thus avoiding speckle generation.

Figure 6 shows more experimental results of image magnified holographic projection under spherical wave illumination. We show three respective reconstructed results of "Baboon" in Fig. 6(b), "Fruits" in Fig. 6(c), and "Parrots" in Fig. 6(d) with the same magnified size (34.56 cm × 19.44 cm) as the "Monalisa" image in Fig. 6(a). Moreover, two animations (Visualizations 1 and 2) are also presented to exhibit the dynamic holographic projection of 1080P high-definition videos. Figures 6(e) and 6(f) are one frame extracted from each animation, respectively. It should be noted that the ringing artifacts appearing at the edge of each reconstructed image are caused by the rectangular band-limit function of convolution operation in ARSS-Fresnel diffraction calculation. The artifacts can be avoided by employing iterative schemes[16] or introducing apodization filtering in CGH calculation.

Finally, another experiment is carried out to further prove the feasibility of projecting magnified color images by the proposed method. We use the similar scheme of the time-sequential control method, as reported in Refs. [13,17] to reconstruct color images. Three phase-only CGHs are calculated independently from the red–green–blue (RGB) component of a color image using the double-step Fresnel diffraction algorithm before they are loaded into the SLM. Three laser beams of red (671 nm), green (532 nm), and blue (473 nm) with a convergent spherical wavefront are used to illuminate the SLM in turn to match the current loaded CGH of the corresponding wavelength. Figures 7(a)–7(c) show the reconstruction of the projected image ("Monalisa") for each used wavelength, and Fig. 7(d) is the mixed color reconstruction. Figures 7(e) and 7(f) are the color reconstructions of the other two images ("Fruits" and "Parrots"). All of the reconstructions in Fig. 7 are captured

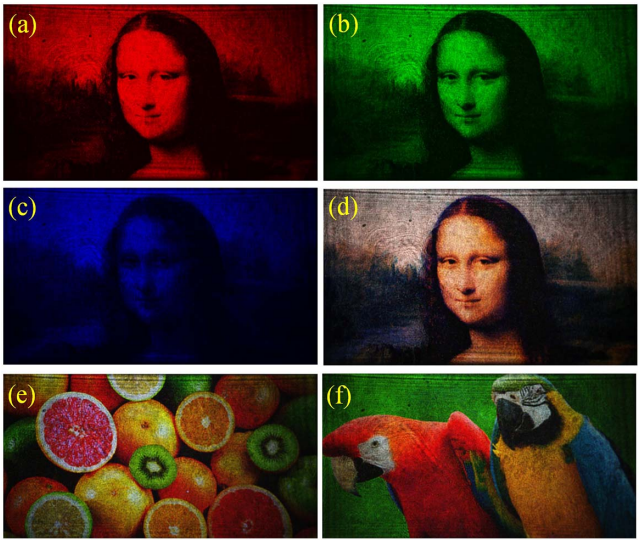

Fig. 7. Optical reconstructions of color projected images. (a)–(c) Individual reconstruction of red, green, and blue components of "Monalisa", respectively. (d)–(f) Color reconstructions of "Monalisa", "Fruits", and "Parrots" with image width of 34.56 cm and image height of 19.44 cm, respectively.

from the projection screen 2 m from the SLM, and they have the same image size of 34.56 cm × 19.44 cm as well as the same resolution of 1920 × 1080.

The significant merit of the proposed method is the suppression of speckle noise through modulating both of the amplitude and phase of the image wavefront; while in the existing methods[9,18], the calculation of CGH using the iterative scheme (i.e., GS algorithm) usually leads to uncontrolled (random) phase distribution and therefore produces speckle noise. We carry out the simulations to theoretically compare the image quality after considering the interference among adjacent image pixels and show the key role of the phase. The first row in Fig. 8 is the reconstruction by the conventional method (GS-based CGH), and the image phase is randomly distributed,

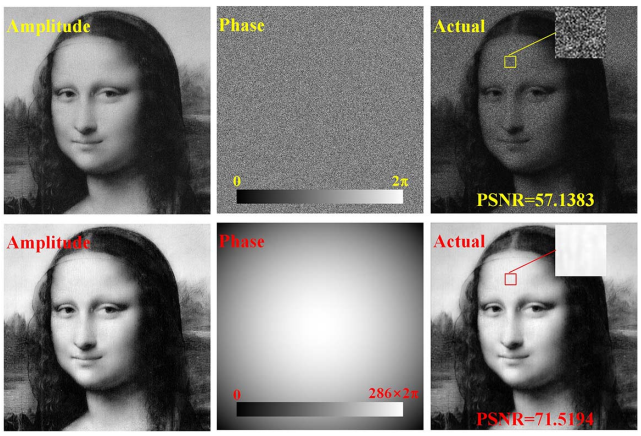

Fig. 8. Comparison of reconstructed images by considering the actual interferences.

whereas the second row is the reconstruction by our method with the designed spherical phase distribution. The actual updated intensities are obtained after calculating the interference among overlapped pixels[5] (adding their complex amplitude values). It can be seen that with the random phase distribution, the actual intensity of the image has great speckle noise due to the destructive interference (discontinues phase jump) between overlapped pixels; but from the result of our method, we can see that with the smooth spherical phase, even if the interference still exists, the image is clear because there is no abrupt phase change between pixels. The quantitative quality of the images is analyzed by calculating speckle contrast[15] in the chosen region (enclosed by solid lines) and peak signal noise ratio (PSNR). The value of speckle contrast is $C = 0.0173$ by the proposed method, while by the conventional method it is up to $C = 0.5278$, proving the speckle reduction effect by the proposed method based on complex amplitude (both of amplitude and phase) modulation.

In this Letter, an image magnified lensless holographic projection system is proposed. The CGH is calculated from the target image by using the double-step Fresnel diffraction algorithm. When using a convergent spherical beam to illuminate the SLM, the diffraction angle of the SLM will be increased physically. The projected image is greatly magnified by breaking the dimension limitation of the Nyquist sampling criterion. Both large-sized monochromatic and color complex amplitude images with suppressed speckle noise are obtained via a lensless optical filtering path. The proposed method has the potential to develop a compact and portable dynamic high-definition holographic projection and display system.

This work was supported by the National Natural Science Foundation of China (NSFC) (Nos. 61605080 and 61775035) and the National 863 Program of China (No. 2015AA016301).

References

1. A. Kaczorowski, G. S. Gordon, and T. D. Wilkinson, Opt. Express **24**, 15742 (2016).
2. E. Buckley, Opt. Lett. **35**, 3399 (2010).
3. E. Buckley, J. Display Technol. **7**, 135 (2011).
4. M. Makowski, I. Ducin, K. Kakarenko, J. Suszek, M. Sypek, and A. Kolodziejczyk, Opt. Express **20**, 25130 (2012).
5. M. Makowski, Opt. Express **21**, 29205 (2013).
6. T. Shimobaba, M. Makowski, T. Kakue, M. Oikawa, N. Okada, Y. Endo, R. Hirayama, and T. Ito, Opt. Express **21**, 25285 (2013).
7. M. Makowski, T. Shimobaba, and T. Ito, Chin. Opt. Lett. **14**, 120901 (2016).
8. T. Shimobaba and T. Ito, Opt. Express. **23**, 9549 (2015).
9. W. Qu, H. Gu, H. Zhang, and Q. Tan, Appl. Opt. **54**, 10018 (2015).
10. T. Shimobaba, T. Kakue, N. Okada, M. Oikawa, Y. Yamaguchi, and T. Ito, J. Opt. **15**, 075405 (2013).
11. N. Okada, T. Shimobaba, Y. Ichihashi, R. Oi, K. Yamamoto, M. Oikawa, T. Kakue, N. Masuda, and T. Ito, Opt. Express **21**, 9192 (2013).

12. R. W. Gerchberg, Optik **35**, 237 (1972).
13. C. Chang, J. Wu, J. Xia, S. Nie, and Y. Qi, Opt. Express **25**, 6568 (2017).
14. O. Mendoza-Yero, G. Mínguez-Vega, and J. Lancis, Opt. Lett. **39**, 1740 (2014).
15. Y. Qi, C. Chang, and J. Xia, Opt. Express **24**, 30368 (2016).
16. T. Shimobaban, T. Kakue, Y. Endo, R. Hirayama, D. Hiyama, S. Hasegawa, Y. Nagahama, M. Sano, M. Oikawa, T. Sugie, and T. Ito, Opt. Commun. **355**, 596 (2015).
17. M. Oikawa, T. Shimobaba, T. Yoda, H. Nakayama, A. Shiraki, N. Masuda, and T. Ito, Opt. Express **19**, 12008 (2011).
18. W. Qu, H. Gu, and Q. Tan, Chin. Opt. Lett. **14**, 031404 (2015).